Signal Processing 20 (1990) 171-182
Elsevier

AUTOMATED BASIN DELINEATION FROM DIGITAL ELEVATION MODELS USING MATHEMATICAL MORPHOLOGY

Pierre J. SOILLE and Marc M. ANSOULT

Unit of Agricultural Engineering, Université Catholique de Louvain, B-1348 Louvain-la-Neuve, Belgique

Received 10 April 1989
Revised 11 August 1989

Abstract. Basin delineation is a major preliminary of hydrologic modeling and watershed management. An efficient method to delineate topographic basins from digital elevation models is presented. It is based upon mathematical morphology and it consists of two major steps. First, remove all the pits within the model by using an original morphological mapping, and second, delineate topographic basins by using morphological thinnings with specific structuring elements. The results are consistent with real terrain features. In a more general way, the proposed methodology illustrates the segmentation approach provided by the morphological watershed mapping.

Zusammenfassung. Die Bassinbeschreibung ist eine wesentliche Vorstufe bei der hydrologischen Modellbildung und der Lenkung der Wasserverteilung. Vorgestellt wird ein effizientes Verfahren zur Beschreibung topographischer Bassins mit Hilfe digitaler Elevationsmodelle. Es beruht auf mathematischer Morphologia, und es besteht aus zwei größeren Schritten. Zuerst werden alle Senken im Modell entfernt, indem eine neuartige morphologische Abbildung verwendet wird. Sodann werden topographische Bassins beschrieben unter Verwendung morphologischer Ausdünnung mit Hilfe bestimmter Strukturierungselemente. Die Ergebnisse sind konsistent mit realen Terraineigenschaften. Die vorgeschlagene Vorgehensweise illustriert auf eine allgemeinere Art den Segmentierungsansatz, den die morphologische Abbildung der Wasserverteilung zur Verfügung stellt.

Résumé. La délimitation des bassins versants est un préalable indispensable à toute modélisation hydrologique. Une méthode efficace de délimitation des bassins versants topographiques à partir de modèles numériques d'altitude est présentée. Cette méthode utilise la morphologie mathématique et comprend deux étapes majeures. Premièrement, supprimer tous les minima locaux internes au modèle en utilisant une transformation morphologique originale et, deuxièmement, délimiter les bassins par une suite d'amincissements morphologiques opérés avec des éléments structurants spécifiques. Les résultats obtenus sont en accord avec les caractéristiques réelles du terrain. D'une façon plus générale, la méthodologie proposée illustre l'approche de la segmentation par la transformation morphologique de la ligne de partage des eaux.

Keywords. DEM, hydrology, image segmentation, mathematical morphology, watershed.

1. Introduction

Topographic and drainage basins are fundamental concepts in earth sciences. The topographic basin of a point P may be defined as the set of topographic surface points whose swiftest descent paths reach P. The drainage basin (i.e., hydrologic meaning) is the topographic area from which all water runoffs finally reach one single given point. Except for special cases, such as some karst landscapes in which leakages and reappearances of subterranean rivers occur, topographic and drainage basins coincide. Basin delineation is important for quantitative studies in hydrology or water resources management.

Digital elevation models (DEMS) are arrays of numbers that represent the spatial distribution of terrain altitudes. The most commonly used data structure for DEMs is the regular square grid in which available elevations are equally spaced in two orthogonal directions. Main data sources for DEMs are ground surveys, existing topographic

maps, photogrammetric stereomodels and surveys done by radar or laser altimeters carried in aircraft and spacecrafts. Although DEMs are now in wide use, topographic basin delineation remains difficult to automatize efficiently. The outline of a basin can be manually digitized from a topographic map and it is recorded in the DEM or any other digital terrain model (DTM).

Manual interpretation of basin boundaries or divide networks from topographic maps is a tedious operation that must be done again for each basin or sub-basin of interest. It is expected that an efficient automated method for basin delineation will more easily allow the production of a basin database within geographical information systems (GIS) and will enhance the use of DTM for watershed research. Consequently, automated delineation using DEMs received recently increasing attention among several research workers (see [1, 5, 8, 13, 14, 21]). After a brief review of these previous works we propose a completely new approach to the question based upon a recent theory of spatial structure analysis called mathematical morphology. Applying this theory to topographic surfaces proves to be very fruitful.

2. Previous works

One of the most cited algorithms which could enable automated basin delineation from DEMs is due to Collins [5]. The first computer operation is to sort the elevation values into an ascending order. The lowest point is the outlet of a topographic basin if it is on the edge of the model; if it is in the body of the model it must be the lowest point of a closed depression. If the second lowest point is not a neighbour of the first, then it must be in a separate basin. The procedure is repeated until each point is assigned to its basin. The methodology appears at first to be susceptible to flat areas and to pits in the elevation data. Pits may have several origins, for example drainage courses are occasionally missed because of the coarse spatial resolution of the grid. Except for volcanic, karst or recently glaciated landscapes, fluvial erosion processes will normally not produce pits at the existing spatial resolution of DEMs and if they occur, they may be regarded as artifacts or data errors. Furthermore, Douglas [6] has demonstrated that the algorithm itself was faulty since of all the points in the same basin, points sorted with respect to their elevation are not necessarily next to each other.

Puecker and Douglas [14] use local analysis of the data. Upward convex pixels are flagged and they are regarded as potential ridge points. As the methodology is highly sensitive to pits and encoding noise, a second processing, rather subjective, is necessary to eliminate improbable points and add missing ones.

Toriwaki and Fukumara [21] first assigned each pixel in one of six different classes (peak, pit, ridge, ravine, hillside and pass) derived from two local topographic properties, the connectivity number and the coefficient of curvature (see also [9]). In a second step, the structural information is extracted from the labelled elements. As in the latter method, some structural information might be missed and false information might be taken into account. Therefore the authors emphasized the incompleteness of the methodology.

Marks et al. [13] delineate topographic basins from slope and exposure digital terrain models derived from DEMs. The method gives good results when artificial pits and flat areas are removed from the initial data (a threshold value to define 'flat' must be found).

Jenson [8] treats each point of the model as the center of a 3×3 spatial window. If a point is a local minimum in comparison with two of its non-adjacent neighbours, it is labelled as a drainage cell. The linkages of drainage cells are established within empirical user-specified distance and elevation ranges. The products of this processing are digital masks of drainage cells and of catchment basins. Without taking into account the restrictions caused by noise and errors in the elevation data, Jenson [8] pointed out that a channel beginning on one side of a hill could grow through a saddle

point and erroneously continue to grow upwards on the other side of the hill.

Band [1] presented a set of local-parallel processing operations to extract divide networks. He emphasizes that artificial pits represent a serious problem to his methodology, especially if the topography is not rugged enough.

3. Mathematical morphology approach

3.1. Preliminaries

Most of the research workers we talked about used at first a local-parallel algorithm (generally defined on a 3×3 moving window) to extract potential divide lines. Then, they successively grow and refine the features into geomorphological reasonable connected divide networks. The major drawback of this methodology remains in the very local approach of the first step because the property to belong to the divide of a given basin does not exist in a 3×3 window since it is subordinated to the location of the outlet of the basin. This remark is also valid in the way by which artificial pits and flat areas are handled. An efficient method of basin delineation using DEMs therefore requires a new approach to the problem. The present approach describes a sequential algorithm based upon mathematical morphology allowing the 3×3 window to grow in size up to the limits of the model.

Mathematical morphology (MM) is the application of lattice theory to spatial structures [17]. Within the scope of this paper we can not develop its theoretical foundations. Articles of Serra [17, 18] and Sternberg [20] are a good introduction in the field. The reference publications of MM are [15, 16]. Most applications of MM are found in the field of digital image processing. Digital binary images were first treated. But now, thanks to the generalization of the theory to n-dimensional spatial structures, digital gray-tone image are handled. Operations of sup ($\bigvee$) and inf ($\bigwedge$) replace the boolean union ($\cup$) and intersection ($\cap$). A DEM can easily be represented as a digital gray-tone image since it is enough to associate each elevation with a gray level proportional to the considered elevation (see Fig. 1). A DEM is therefore thought of as a numerical or 'gray-tone' function (f) defined over a subset (D) of the 2-dimensional digital space ($\mathbb{Z}^2$). The 'gray' at any point $x \in D$ being the altitude at this point. Although digital MM is more powerful when using the hexagonal grid we will restrict our attention to

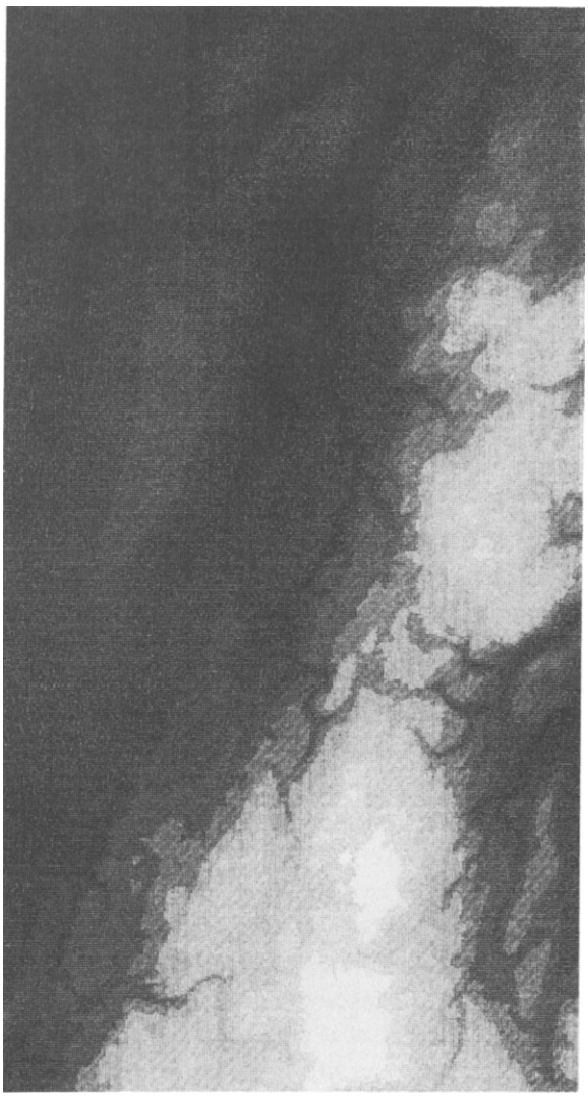

Fig. 1. DEM represented as a digital gray-tone image. The model has an equal X-Y resolution of 50 m and covers a surface of 312 km^2 in the Canton de Vaud, Switzerland. Terrain altitudes range from 432 to 937 meters.

the regular square grid in spite of methods to turn a square into a hexagonal grid [19] since most DEMs are produced according to the square grid.

According to MM, graphs of gray-tone functions are often considered as imaginary topographic reliefs on which several features may be defined. This analogy is exclusively used to apprehend theoretical concepts better, but, in the scope of our research, this analogy becomes reality and it is worth drawing our attention.

Serra [15] defines a sink (or minimum) of a function f in terms of cross-sections as follows: let $X_t(f)$ be a cross-section of f at level t, i.e., $X_t(f) = \{x \in \mathbb{Z}^2 | f(x) \leq t\}$; then a connected component $M_t(f)$ of the cross-section $X_t(f)$ is a sink if for every $x \in M_t(f)$ and for every $t' < t$ we have $x \notin X_{t'}(f)$, i.e.,

$$M_t(f) \text{ sink} \Leftrightarrow x \in M_t(f) \Rightarrow x \notin X_{t'}(f) \quad \forall t' < t.$$

The sinks of f are the summits of $-f$ and conversely (dual notions). By themselves, summits and sinks do not associate any knowledge about their surroundings, therefore notions of catchment basins and hills were proposed to define the topological equivalence class for functions.

The catchment basin of a sink M of a function f is the sets of points $(x, f(x))$ which belongs to the boundary of the umbra $\partial[U(f)]$ (i.e., the graph of the function) whose lines of swiftest descent only reach M. Those points of $\partial[U(f)]$ which do not belong to a catchment basin are called the divides (see Fig. 2). Remark that divides are made of points generating two lines of swiftest descent but which reach two separate sinks.

The catchment basin notion expressed here may be considered as the generalization of the binary concept of SKIZ (skeleton by influence zone): the catchment basins of a gray-tone function are the influence zone of its minima. The projection of the divides onto the binary plane, which is called the support of the divides, creates a tessellation of the plane. Divide mappings (also named watershed mappings) are very effective in contour detection and picture segmentation [2]. Contours are defined as the divides of the variation function (gradient modulus) of the gray-tone function.

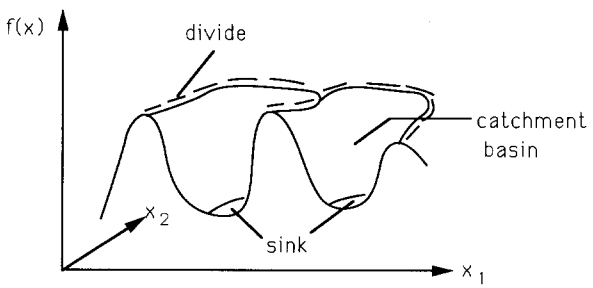

Fig. 2. Noteworthy features of a gray-tone function: sinks, catchment basins and divides (dual features are summits, hills and channels, respectively).

The basic difference between notions of catchment and topographic basins is that a catchment basin (i.e., MM meaning) is necessarily a zone of influence of a minimum, whereas a topographic basin can represent the zone of influence of any topographic surface point.

3.2. Algorithm to delineate catchment basins of DEMs

Although the above-mentioned notions are clearly descriptive, MM provides tools to extract the catchment basins of a function. Beucher and Lantuéjoul [3], and more recently Beucher and Vincent [4], define a way to build the divides of a function using the propagation graph or flood process idea. Each basin is flooded and every time an overflow occurs a dam can be built on $\partial[U(f)]$ to prevent an overflow. When the dam has drawn a closed contour, we get the boundary or divide of the catchment basin. Therefore, watersheds of a function are progressively constructed by using the geodesic SKIZ (i.e., GSKIZ) of a level inside the next one. The GSKIZ is computed thanks to conditional binary thickenings.

This procedure processes the successive cross-sections of the function and this might be a major drawback when dealing with functions made up of numerous levels like DEMs. Fortunately, morphological mappings called thinnings allow to

derive the divides without thresholding steps. Let us recall the definition of lower thinnings (i.e., thinnings with flat structuring elements). Let $T = (T_1, T_2)$ a flat structuring element, the datum being two sets T_1 and T_2. The thinning of a function f by T, written $f \circ T$, is a mapping which provides a new function g, where $g = f \circ T$ is defined as follows:

$$\text{if } \sup_{y \in (T_2)_x} f(y) = f(x) \oplus \check{T}_2 < f(x)$$

$$\leqslant \inf_{z \in (T_1)_x} f(z) = f(x) \ominus T_1$$

$$\text{then} \quad g(x) = f(x) \oplus \check{T}_2$$

$$\text{otherwise} \quad g(x) = f(x).$$

$(T_i)_x$ means the origin of T_i is set on x, $\oplus$ is the symbol used for the morphological dilation (same as for Minkowski addition) and $\ominus$ for morphological erosion (same as for Minkowski subtraction).

$\check{T}_i = \bigcup_{y \in T_i} \{-y\}$ is the transposed set of T_i.

Seeing that divides (and channels) characterize the homotopy of gray-tone functions, homotopic thinnings preserve the divides. Therefore divides of a function are included in its skeleton as the skeleton is performed by processing homotopic thinnings until idempotence has been reached. Ridges are defined as points generating two lines of swiftest descent but, contrary to divide points, these lines reach the same sink. Ridges of a function are also included in its skeleton.

Beucher [2] has reached the conclusion that the divides of a function are nothing else than the closed arcs of its skeleton. In other words, if we eliminate the 'barbs' of the skeleton (by pruning until idempotence), we obtain the divides. But the composition of two idempotent mappings is not necessarily idempotent. Therefore, we propose to proceed in the following way: a sequence of homotopic thinnings until idempotence followed by a sequence of prunings until idempotence, but the whole process also has to be repeated until idempotence. In Fig. 3 it is shown that the two first sequences are not idempotent. Figure 3(a) is obtained by homotopic thinnings until idempotence and Fig. 3(b) by pruning it until idempotence. Obviously, if a new sequence of homotopic thinnings is performed on Fig. 3(b), values at '8' will be set to '7'. The algorithm is illustrated by a flow chart in Fig. 4. M has a homotopic configuration used to complete skeletons and E has an non-homotopic one to prune or clip skeletons (cf. 'Golay alphabet', [7, 15]). $\{M\}$ or $\{E\}$ means that an iterative or sequential mapping with the successive rotations of M or E must be accomplished. Figure 5 presents M and E configurations within the square grid [10].

(a)

13	14	15	16	14	15	16	17	14
14	7	7	7	11	6	6	6	13
14	7	7	7	10	6	6	6	13
14	7	7	7	11	6	6	6	14
15	7	11	8	12	13	11	12	13
16	7	10	8	8	12	9	9	13
16	7	12	8	8	15	9	9	14
15	16	15	15	17	18	17	16	16

(b)

13	13	13	13	13	13	13	13	13
13	7	7	7	10	6	6	6	13
13	7	7	7	10	6	6	6	13
13	7	7	7	10	6	6	6	13
13	7	**8**	**8**	10	11	11	11	13
13	7	**8**	**8**	**8**	11	9	9	13
13	7	**8**	**8**	**8**	11	9	9	13
13	13	13	13	13	13	13	13	13

Fig. 3. (a) Sample data of a skeletonized image. (b) Resulting data when pruning (a) until idempotence.

To avoid side-effects a one-thickness frame of value i ($i > f(x)\ \forall x \in D$, where D is the spatial field of f) must be added around the spatial field of the model. This frame acts as a great divide surrounding the model. At the end of our processing we get a new gray-tone function $h(x)$ which has the following features. Each catchment basin

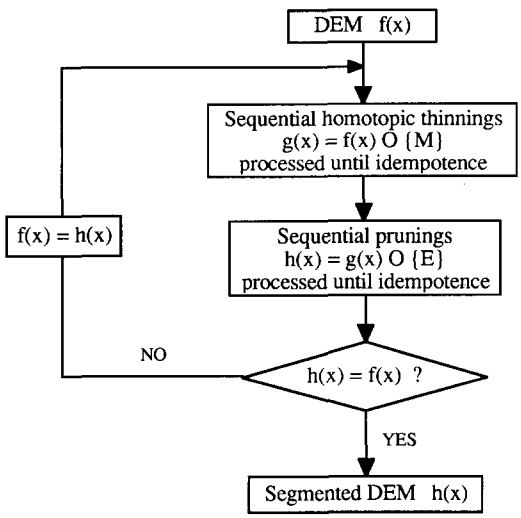

Fig. 4. Algorithm to delineate catchment basins of a gray-tone image. Notice that the whole process is repeated until idempotence.

$$M = \begin{matrix} 0\ 0\ 0 \\ .\ 1_0\ . \\ 1\ 1\ 1 \end{matrix} \quad \text{and} \quad \begin{matrix} .\ 0\ . \\ 0\ 1_0\ 1 \\ .\ 1\ 1 \end{matrix} \quad \text{and their rotations of } \Pi/2, \Pi, 3\Pi/2$$

$$E = \begin{matrix} .\ 0\ . \\ 0\ 1_0\ 0 \\ .\ .\ . \end{matrix} \quad \text{and their rotations of } \Pi/2, \Pi, 3\Pi/2$$

Fig. 5. Flat structuring elements used to skeletonize $\{M\}$ and to prune $\{E\}$ digital gray-tone images within the square grid (4-connected graph). The zero index is used to locate the origin of the structuring element. '1' is used to specify elements belonging to T_1 (i.e., M_1 or E_1) and '0' to T_2 (i.e., M_2 or E_2). Points (.) means that the element belongs neither to T_1 nor to T_2.

Fig. 6. Segmentation of the DEM presented in Fig. 1 into its catchment basins by using the algorithm presented in Fig. 4.

is set at the height of its minima and the divides are not destroyed; each path lying between two of its multiple points is put down to the lowest terrain elevation along the considered path. The former feature is due to the homotopic thinning and the latter to the pruning sequences.

The application of the algorithm to a DEM has led to the image $h(x)$ shown in Fig. 6. At first glance there seems to be something wrong with the algorithm because there are many minute catchment basins inside the DEM, whereas without closed depressions (like quarries, volcano, craters, . . .) each basin should have an outlet along the boundary of the model. Notice that these outlets become sinks since the model is surrounded by a divide (i.e., the frame of value i added to avoid side-effects). In fact, the abundance of small catchment basins inside the DEM was expected. Remember that when discussing about previous works all authors got some troubles with pits inside their DEMs. There is no way to escape this, since each pit has a zone of influence (its catchment basin) which will naturally be detected by the

algorithm. Therefore pits in the elevation data elucidate the minute tessellations of $h(x)$.

3.3. Algorithm to remove pits within DEMs

To get a partition of the model which fits better real terrain features, a method to remove all the pits within the model must be developed. Most research workers filter elevation data with techniques like convolutions, median filters, ... These techniques have a major drawback in this case: they are not selective since nearly all data are altered and this smoothes topography leading to a loss of information. Furthermore, some pits remain after the treatment. Morphological filters, like openings, closings or one combination of one and another (see [12, 16]) may also be applied to the data. These filters are more selective (besides they are indempotent). Nevertheless, their application to the problem we are dealing with has led to entirely unsatisfactory results. For example, an elementary closing removes all the pits defined on a 3×3 window, but it also creates big pits by walling up narrow valleys. Another technique had to be developed. The algorithm, again based upon MM, is presented below.

As mentioned above, a reasonable assumption is to consider all pits within DEMs as artifacts created during the digitizing process. Now, suppose we are dealing with a DEM free of closed depressions or pits.

Let H be the elementary isotropic convex structuring element of the grid (Fig. 7),
D, the spatial field of a function f,
$f(x)$, terrain elevations at spatial coordinates $x(x \in D)$,
$X_t(f) = \{x | f(x) \leq t\}$, a cross-section of f at level t,
$\partial D^c = (D \oplus H)/D$, the boundary ($\partial$) of the complement (^{c}) of the spatial field (D) of f.
iff f is free of minimum
then $[\partial D^c \cup X_t(f)]$ is one and only one connected component for every t.

$$\begin{array}{ccc} . & 1 & . \\ 1 & 1 & 1 \\ . & 1 & . \end{array} \qquad \begin{array}{ccc} 1 & 1 & 1 \\ 1 & 1 & 1 \\ 1 & 1 & 1 \end{array}$$

(a) **(b)**

Fig. 7. Elementary isotropic convex structuring element H within the square grid. (a) 4-connected graph. (b) 8-connected graph.

(Notice that $X_t(f)$, D and ∂D^c are digital binary sets). '/' symbolises the difference between sets.

In other words, each connected component $Y_t(f)$ of $X_t(f)$ hits the boundary of the spatial field of f, i.e.,

$$\{Y_t(f) \cap [D/(D \ominus H)]\} \neq \emptyset$$
$$\forall Y_t(f) \in X_t(f).$$

If f has pits, this property will not be checked for every t, since when a pit occurs at level i it generates a connected component $M_i(f)$ of $X_i(f)$ which does not hit the boundary of D, i.e.,

$$\{M_i(f) \cap [D/(D \ominus H)]\} = \emptyset$$
$$\Leftrightarrow M_i(f) \text{ is a sink.}$$

We take advantage of this property to fill the pits (see Fig. 8). The core of our algorithm is the conditional dilation (i.e., $B = (A \oplus H) \cap X_t(f)$) processed until idempotence. This mapping can not reach the connected components which are not connected to ∂D^c (i.e., pit locations) and it is used to increment specifically the pit elevation until an outlet is created at the lowest point of each divide (it might be called the 'pour point', see Fig. 9).

Again the gray-tone function can be handled immediately instead of working on its cross-sections by doing erosions until idempotence of a marker function $m(x)$ conditionally to $f(x)$ (i.e., conditional gray-tone erosion). One may easily find that the marker function should be as follows:

$$m(x) = 0 \quad \text{iff} \quad x \in (D \oplus H)/D,$$
$$m(x) = \sup\{f(y) | y \in D\}$$
$$\text{iff} \quad x \in D.$$

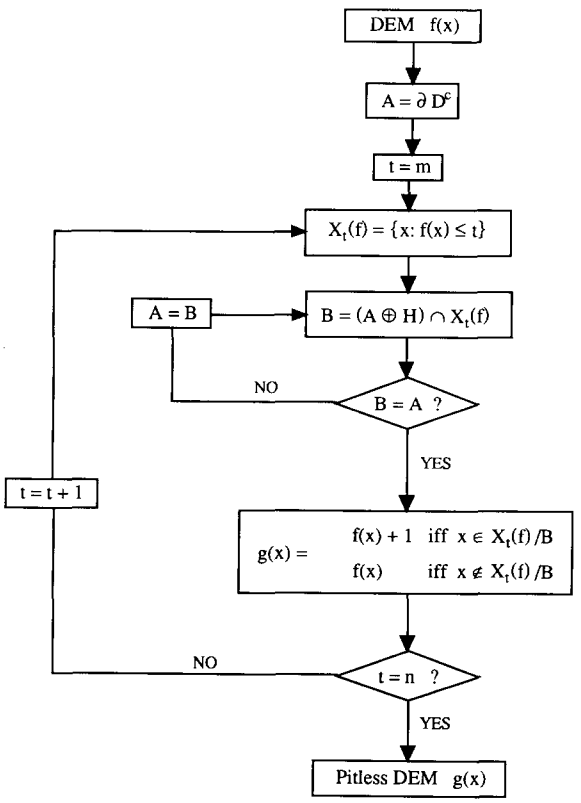

Fig. 8. Flow chart of the algorithm to fill pits of DEMs (binary version). $f(x)$ is the input DEM, $g(x)$ is the output DEM ($m \leq f(x) \leq n$, integers). D is the spatial field of the input DEM.

The principle is illustrated in Fig. 10 for a one-dimensional function and a flow chart is given in Fig. 11. Notice that the algorithm is a closing (algebraic sense) since it is an extensive, idempotent and growing mapping.

Location of the sinks is easily done by subtracting the initial DEM $f(x)$ from the pitless DEM $g(x)$. The non-zero values correspond to the bottom of each closed depression which were incremented until an overflow occurs. As indicated in Fig. 12, pits are mainly located in valley floors and other flat areas of the DEM. This could have been foreseen since it is where the signal-to-noise ratio is the least favorable: when slopes are gentle, a small error on elevation measurement may be enough to produce a closed depression, while on steeper slopes, a pit does not result.

(a)

11	14	9	9	7	8	8
14	**15**	**15**	**14**	**12**	**13**	12
13	**15**	11	11	11	**12**	11
13	**16**	11	9	8	**10**	9
13	**17**	11	9	11	**12**	11
13	**13**	**12**	**14**	**12**	**12**	11
12	12	11	11	11	11	11

(b)

11	14	9	9	7	8	8
14	**15**	**15**	**14**	**12**	**13**	12
13	**15**	11	11	11	**12**	11
13	**16**	11	10	10	10	9
13	**17**	11	10	11	**12**	11
13	**13**	**12**	**14**	**12**	**12**	11
12	12	11	11	11	11	11

Fig. 9. (a) Pit with its divide in bold. (b) Numerical values by applying algorithm to remove pits on (a). The 'pour point' is no longer in bold.

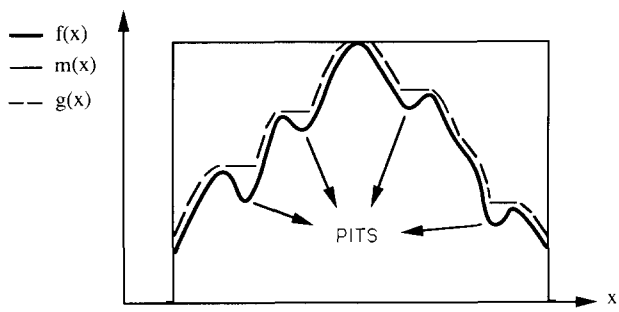

Fig. 10. Erosion until idempotence of a marker function $m(x)$ conditionally to $f(x)$: at each step, $\sup[m \ominus B, f]$, where B is the linear elementary structuring element, is computed. Resulting function is $g(x)$. Note the removal of the pits.

3.4. Results and comments

Now, we are able to automatically delineate topographic basins of DEMs under the assumption that all the pits within DEMs may be thought of as artifacts due to the digitizing process. This being granted, one must proceed as follows: first, apply the algorithm to remove all the pits within the DEM (see Section 3.3); second, apply the divide

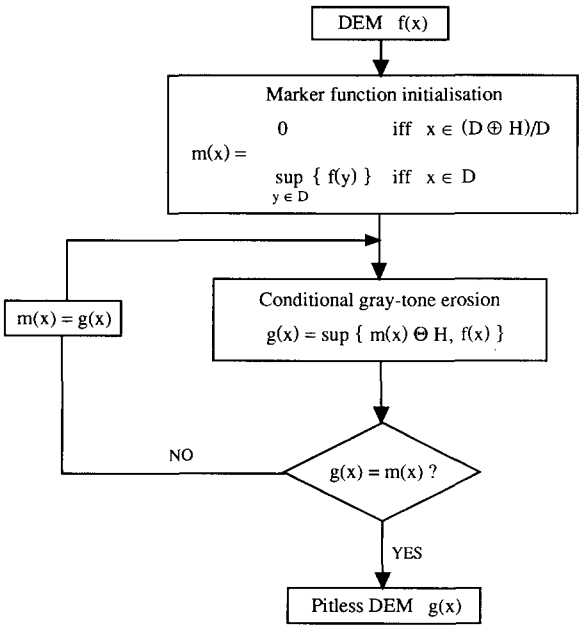

Fig. 11. Flow chart of the algorithm to fill pits of DEMs (gray-tone version).

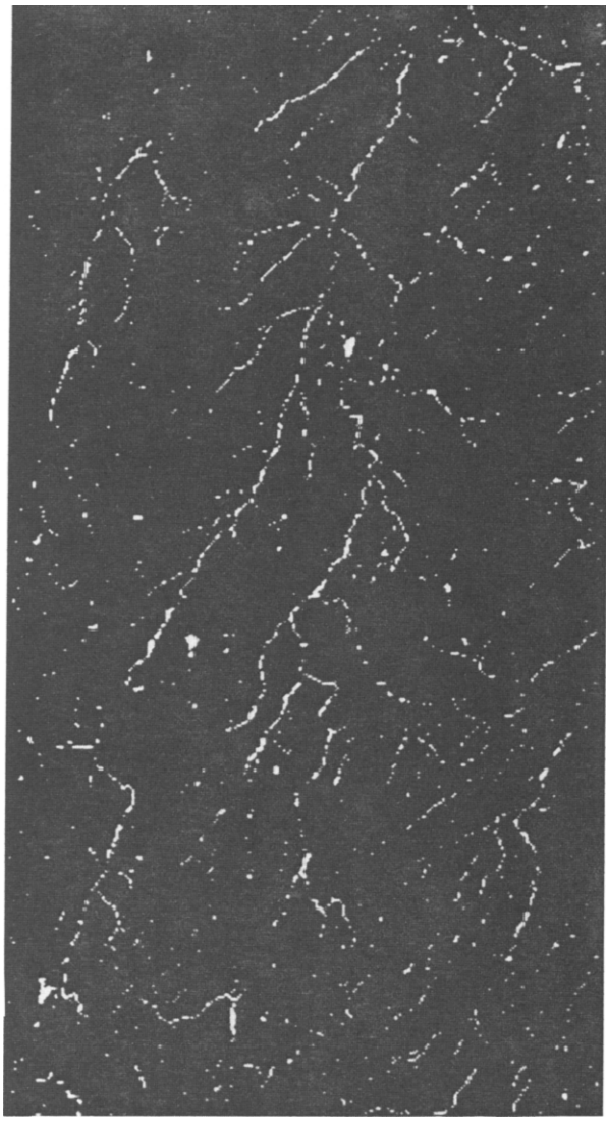

Fig. 12. Pit locations of the DEM presented in Fig. 1.

or watershed mapping to delineate topographic basins of DEMs (see Section 3.2). Note the independence between the two steps. The procedure allows to segment the DEM into its greatest topographic basins since the considered outlets are distributed along the edge of the model. The output gray-tone image is presented in Fig. 13 and it fits to 'real' terrain features as it can be seen in Fig. 14 where divides are superimposed with the initial DEM. If one wants to relate the catchment basin to a particular point within the pitless model, it is enough to reduce the elevation of the point to create an artificial pit. This allows to get topographic and catchment basins to coincide (see below).

The greatest basin represented in Fig. 14 is the basin of the Mentue river and it has been studied in details by Zwahlen [22]. The basin boundary related to a particular gauging station was derived from topographic maps. In Fig. 15, the basin boundary presented by Zwahlen [22] is compared to that obtained from the present procedure after having created an artificial pit at the location of the gauging station in the pitless DEM. Notice that the basin of the Mentue is devoid of closed depressions and the fore-mentioned assumption can be applied without restrictions. The comparison shows that the two boundaries do not coincide all along although deviations remain small. These deviations are mainly due to the differences between the continuity of the real terrain and the discrete nature of DEMs. It must be

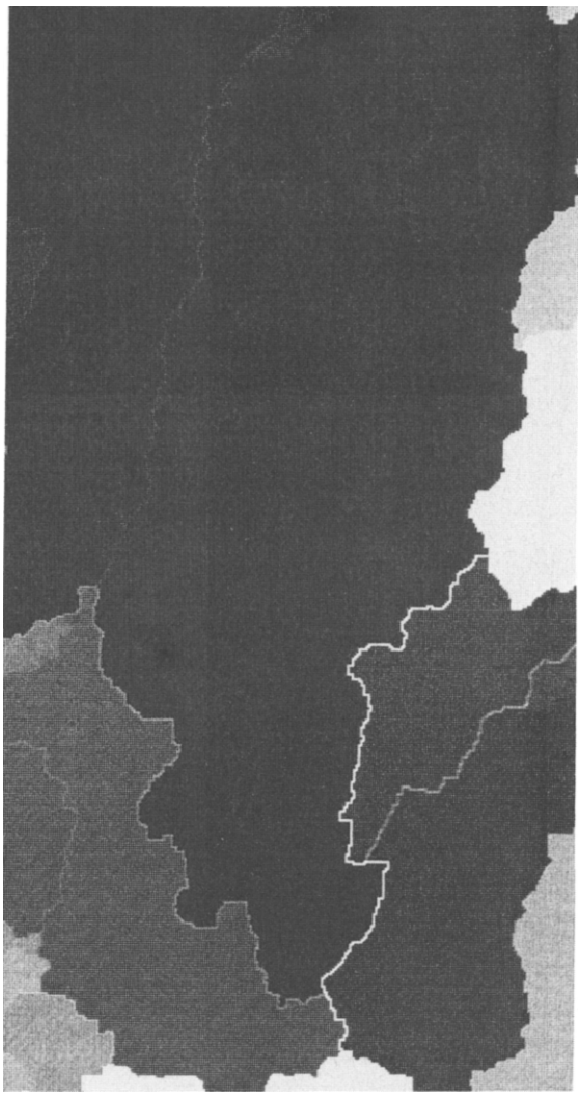

Fig. 13. Catchment basins and divides of the DEM by using the proposed methodology.

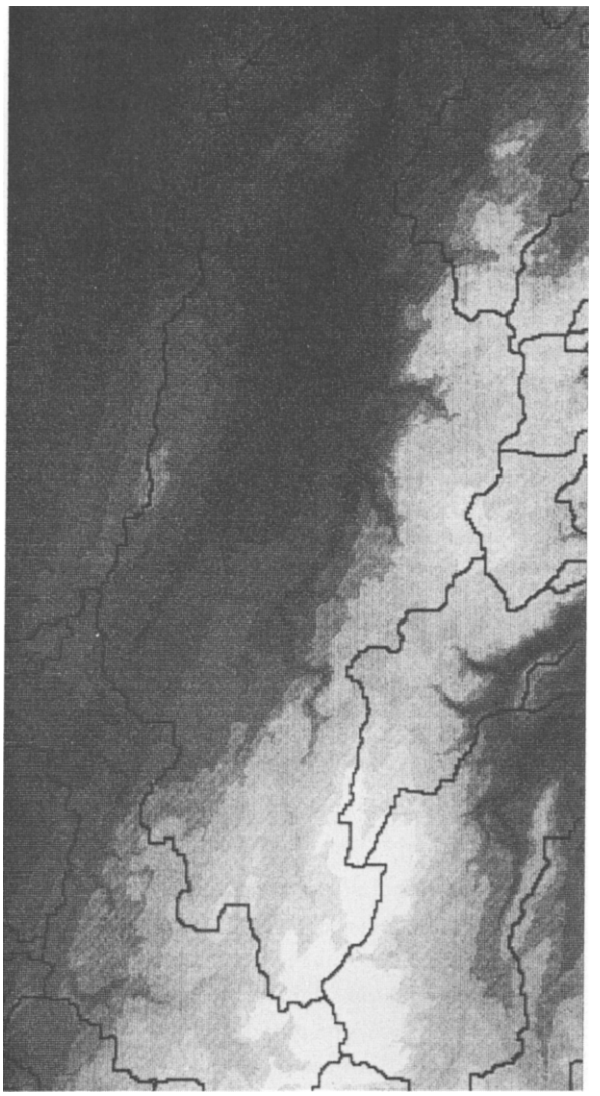

Fig. 14. Divides in superimposition with the DEM.

specified that the values of the initial DEM, which are integers ranging from 432 to 937, had to be reduced to integers ranging from 0 to 255 (hardware constraint). This operation decreases the resolution on the elevation data by more than 2 leading to a loss of accuracy when delineating basin boundaries. But cell size is probably the most important factor. In fact, basin boundaries are related to fractal geometry like any other geographic line (Mandelbrot [11]). It is easy to understand that a basin boundary drawn from a map scaled to 1:1 000 000 will be different if the map is scaled to 1:1000. In the same way, a divide extracted from a DEM which has a spatial resolution of 100 meters will not be the same if it is 1 meter. The greater the scale of the map or the spatial resolution of the grid is, the greater the length of the divide line will be. This is a very important notion since it shows that topographic basin boundaries are scale dependent features.

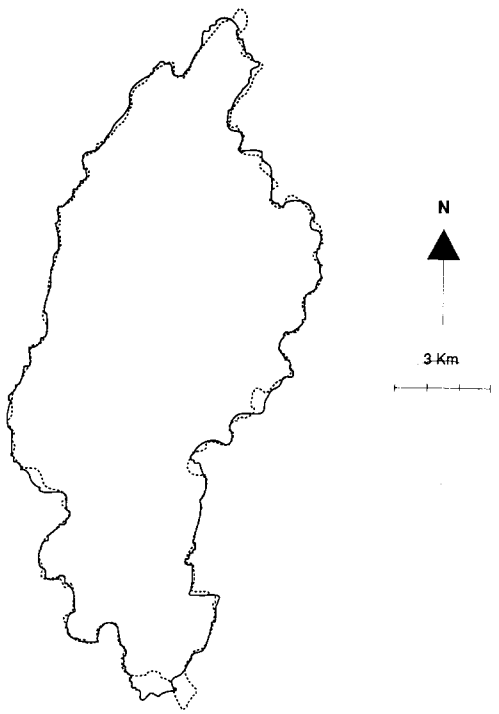

Fig. 15. Comparison between basin boundary of the Mentue river derived from topographic maps and ground surveys (dotted line) and from a DEM by using the developed procedure (continuous line).

4. Conclusions

Applying MM to DEMs turns out to be very fruitful since an original and sound method for delineating topographic basins from DEMs has been developed. Contrary to all previous works, it deals with flat areas and artificial pits. All the processing is performed by working directly on the gray-tone function.

In a more general way, this manuscript illustrates the segmentation approach provided by the morphological divide or watershed mapping [4]. When applying it to an image or, as usually, to the gradient of an image, one is disappointed by the resulting oversegmentation caused by the presence of insignificant minima. Therefore the essential prerequisite of an efficient segmentation using the watershed mapping consists in removing these minima while keeping the others. Marker functions

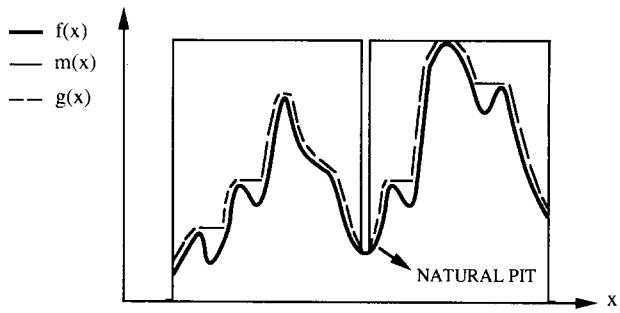

Fig. 16. The marker function is modified to prevent the removal of a natural pit (e.g., a volcano crater). See also Fig. 10.

are very effective at this stage. In practice, however, the construction of marker functions is the most difficult step of this segmentation approach. The strength of this methodology applied to DEMs rests on the near independence between the marker function and the DEM: it suffices to assume that pits represent artifacts to build unambiguously the marker function. Finally, the sole working hypothesis of this research could be removed if natural pits could be distinguished from artificial ones (e.g., by size or shape criteria). This would allow to modify the marker function in order to prevent the removal of natural pits (see Fig. 16).

This research is expected to increase the use of DEMs for any terrain phenomenon that is related to watershed location. It has also demonstrated that MM is well suited for analysing topographic surfaces, the spatial structure above all else. In this perspective, other terrain features like ridges, channels, ... could also be derived from morphological mappings.

Acknowledgments

The authors would like to thank Professors Louis de Backer and Jules Wilmet for providing valuable advice and encouragement, as well as Pascal Jacques for his introductory help to digital image processing programming. We also would like to thank the Institut de Géophysique de l'Université de Lausanne (Switzerland) for placing their DEM of the Mentue at our disposal.

References

[1] L.E. Band, Topographic partition of watersheds with digital elevation models, *Water Resources Research*, Vol. 22, No. 1, 1986, pp. 15-24.

[2] S. Beucher, Watersheds of functions and picture segmentation, *Proc. IEEE Internat. Conf. Acoust. Speech Signal Process. 82*, Paris, 3-5 May 1982, pp. 1928-1931.

[3] S. Beucher and C. Lantuéjoul, Use of watersheds in contour detection, *Internat. Workshop on Image Processing*, CCETT, Rennes, France, 12 pp.

[4] S. Beucher and L. Vincent, Introduction aux outils morphologiques de segmentation, *J. Spectroscopie Microscopie Electronique*, to be published.

[5] S.H. Collins, Terrain parameters directly from a digital terrain model, *The Canadian Surveyor*, Vol. 29, No. 5, 1975, pp. 507-518.

[6] D.H. Douglas, Experiments to locate ridges and channels to create a new type of digital elevation model, *Cartographica*, Vol. 23, No. 4, 1986, pp. 29-61.

[7] M.J. Golay, Hexagonal parallel pattern transformations, *IEEE Trans. Comput.*, Vol. C-18, No. 8, 1969, pp. 733-740.

[8] S.K. Jenson, Automated derivation of hydrologic basin characteristics from digital elevation model data, *Proc. Auto.-Carto. Digital Repres. Spatial Knowledge*, 1984, pp. 301-310.

[9] E.G. Johnston and A. Rosenfeld, Digital detection of pits, peaks, ridges and ravines, *IEEE Trans. Systems Man. Cybernet.*, Vol. SMC-5, 1975, pp. 472-480.

[10] S. Levialdi, Parallel pattern processing, *IEEE Trans. Systems Man Cybernet.*, Vol. SMC-1, 1971, pp. 292-296.

[11] B.B. Mandelbrot, *The Fractal Geometry of Nature*, Freeman, New York, 1983.

[12] P. Maragos and R.W. Schafer, Morphological filters—Part I: their set-theoretic analysis and relations to linear shift-invariant filters, *IEEE Trans. Acoust. Speech Signal Process.*, Vol. ASSP-35, No. 8, 1987, pp. 1153-1169.

[13] D. Marks, J. Dozier and J. Frew, Automated basin delineation from digital elevation data, *Geo-Process.*, Vol. 2, 1984, pp. 299-311.

[14] T.K. Puecker and D.H. Douglas, Detection of surface-specific points by local parallel processing of discrete terrain elevation data, *Comput. Graphics Image Process.*, Vol. 4, 1975, pp. 375-387.

[15] J. Serra, *Image Analysis and Mathematical Morphology*, Academic Press, London, 1982.

[16] J. Serra, *Image Analysis and Mathematical Morphology, Volume 2: Theoretical Advances*, Academic Press, London, 1988.

[17] J. Serra, Introduction to mathematical morphology, *Comput. Vision Graphics Image Process.*, Vol. 35, 1986, pp. 283-305.

[18] J. Serra, Morphological optics, *J. Microscopy*, Vol. 145, Pt 1, 1987, pp. 1-22.

[19] J. Serra and B. Laÿ, Square to hexagonal lattices conversion, *Signal Process.*, Vol. 9, No. 1, 1985, pp. 1-13.

[20] S.R. Sternberg, Grayscale morphology, *Comput. Vision Graphics Image Process.*, Vol. 35, 1986, pp. 333-355.

[21] J. Toriwaki and T. Fukumara, Extraction of structural information from grey pictures, *Comput. Graphics Image Process.*, Vol. 7, 1978, pp. 30-51.

[22] F. Zwahlen, Contribution à l'étude hydrologique du bassin de la Mentue, problème de la cartographie des éléments du bilan hydrique, Thèse présentée à la Faculté des Sciences de l'Université de Lausanne, 1981.